8

Control of Lightweight Manipulators Based on Sliding Mode Technique

Jingxin Shi, Fenglei Ni and Hong Liu
Institute of Robotics, Harbin Institute of Technology, Harbin, Hilongjian Province
China

Abstract
This chapter focuses on the dynamic control issues of lightweight robots as well as flexible joint robots. The goal is to increase the bandwidth and the accuracy of the trajectory tracking control. Besides the joint flexibility, the control design considers the dynamics of the electric motor in AC-form i.e. the three phase permanent magnet synchronous motor (PMSM). The final system model is a fifth order non-linear system. Based on the theory of integral sliding mode control a robust control approach for the trajectory tracking control of rigid-body robots is presented at first. This control approach has pole-placement capability despite system uncertainties. The controller is then used as the outer position controller for the control of flexible joint robots. To handle the joint flexibility, singular perturbation approach is employed, resulting in reference currents for the inner current control loop of joint motors. For the current control, sliding mode PWM technique is used to overcome the disadvantages of conventional open-loop PWM. The developed control algorithms are simple enough for practical implementation and verified by simulation studies based on a dynamic model consisting of a two-link flexible joint robot with two joint motors.

1. Introduction

The development of robotics in the past few years has been extended from the earlier standard applications of industrial robots to new fields such as service, space robotics and force-feedback systems. The design goals of the new robot generation aim at lightweight, high output torque, high speed, multi-sensory and high degree of learning capability. Such advanced features inevitably increase the complexity of the dynamic control tasks. For a lightweight robot, to avoid the disturbance torque, such as backlash etc., gearboxes with harmonic drive are often involved; this leads to flexibility in robot joints in turns. It is recognized meanwhile that the dynamic control of real world lightweight robots to reach a high system bandwidth is a challenging topic to the current development of robotics and available control technologies. The key factor which limits the system bandwidth is the "high-order", originated from the joint flexibility and the dynamics of the electric motors.
It is recognized that the state-space approach based on the feedback linearization is not adequate for the control of real world lightweight robots and even not adequate for the

control of any high-order non-linear uncertain system, despite being able to assign the closed-loop poles arbitrarily. Another methodology to control the lightweight robots is to decompose the high-order system into two or more lower order sub-systems. There are some remarkable advantages with this methodology: control approaches for rigid-body robots may be used further; the higher order time derivatives of the link position such as acceleration and jerk may be avoided; and, it is easier to set the control system into operation. One of the control methods under this category is the famous singular perturbation approach (as well as the integral manifold approach) which takes the joint torque sub-system as an algebraic system for the link position control and adds some damping for the fast motion in the joint torque. In this way, the joint torque dynamics are resolved without the need of exact tracking of a joint torque reference trajectory. Because the joint torque dynamics are almost "by-passed", this approach may possess a higher bandwidth for the link position control than the pure cascaded control structure with a joint torque control loop being inserted between the link position and motor current control loops. As a result, the composed control structure of singular perturbation approach for the joint torque dynamics can be interpreted as a feed-forward control of the joint torque added by some damping to the fast motion in the joint torque. Singular perturbation approach is verified as a simple and effective approach to stabilize the joint flexibility.

A pioneer of flexible joint robot control is Professor Mark W. Spong when he worked for University Illinois from1984 to 2008. He established the famous Spong-model for flexible joint robots and studied almost all aspects for the dynamic control of this kind of robots.

In the following, some important publications will be citied to clarify the main stream of the dynamic control issues.

The concept of new generation robotics with modular structure was proposed by Hirzinger's group as the spring-out of space robotics technologies (Hirzinger et al., 1994; Gombert et al., 1995). Later on, the concept was modified to the goals of having human arm performance with very high load/own-weight ratio as well as torque sensing and feed-back capability, with certain degree of human intelligence, providing new possibilities for space, medicine and other applications (Stieber et al., 2000; Schmidt, 2000; Hirzinger et al., 2001; Hirzinger et al., 2001; Koeppe & Hirzinger, 2001).

The fundamental control approaches for flexible joint robots were established by Spong (Marino & Spong, 1986; Spong, 1987; Spong, 1988; Spong, 1989). Since then, numerous theoretical results are developed and mainly tested with computer simulation. The developed control methods include:

(a). state-space approach based on the feedback linearization
(b). singular perturbation approach as well as integral manifold approach
(c). dynamic feedback linearization approach
(d). adaptive control technique
(e). simple PD control
(f). PD control + joint torque feedback
(g). passivity based control approach

As proposed in (Spong , 1987), for the state-space approach based on the feedback linearization, even using simplified robot model, the resulting control algorithm may not be realizable due to the state transformation and the inverse calculation of the control inputs. The control algorithm depends on the robot parameters, which are generally unknown.

As stated before, singular perturbation approach is a promising approach by solving the control problem in two time scalars: a fast joint torque damping term for the fast mode of the joint torque dynamics, and a slow joint torque feed-forward term for the outer position control loop (related to the rigid body dynamics of the robot arm) (Spong, 1987; Readman & Mark, 1994).

De Luca involves the previous system information to form the so-called dynamic feedback linearization (De Luca et al., 1998). He uses not only the actual states of the robot dynamics, but also the past states; no global state transformation is required. The resulting control structure is of 2n(n-1) order (with n being the number of robot joints). (De Luca et al., 1998) won a best paper awarded during conference IRCA98 due to the theoretical contribution.

In order to remove the requirement of exact knowledge about robot parameters, adaptive control techniques for flexible joint robots have been developed (Spong, 1989, Lin et al., 1995). These approaches can be viewed as an extension of adaptive control for rigid body robots (Slotine & Li, 1987). Though theoretically looks well, this method met the problem of over complexity for the practical implementation.

Engineers tried PD (or PID) controllers, traditionally used for industrial robots, adding some damping term for the joint flexibility. Stability proof for such control systems, if it is possible, is more involved than that of using extensive model information. Starting from (Arimoto, 1994), which provides the theoretical justification for the PD controller still used in most industrial robots, Tomei (Tomei, 1991) proved the stability of PD control with gravity compensation also for flexible joint robots. However, the stability proofs are only valid for the link position regulation and not for the trajectory tracking control.

Albu-Schaeffer (Albu-Schaeffer & Hirzinger, 2000) proposes an intermediate approach between the theoretical and the practical solutions for the link position control i.e. PD control + joint torque feedback. He uses a simple control structure in the form of joint state feedback with gravity compensation, applicable for a lightweight robot with 7DOF. A stability proof based on Lyapunov theory was provided as well. Also here, the stability proof is valid only for the case of point-to-point motion of the robot arm and not valid for the trajectory tracking control.

Ott (Ott, 2008) studied and tested several control approaches systematically including the passivity based control approach. It comes to the conclusion that the passivity based control approach doesn't show an improved performance for the trajectory tracking control despite of some other advantages. Similar to the works by Albu-Schaeffer (Albu-Schaeffer, 2002), the proposed control algorithms by Ott need often the system parameters which may not be available for general purpose lightweight robots.

In (Ozgoli & Taghirad, 2006) an extensive survey about the control of flexible joint robots is given in which 173 papers from different aspects of the control issue are cited.

It is recognized meanwhile that to design a good control system, the controller designer must have a deep understanding about the physic plant to be controlled, independent from which control approach is applied. As a result, at least a rough model for the controlled plant is required, though there are some unmodeled dynamics, external disturbances and parameter uncertainties associated with this rough model. As a candidate of physic oriented control theories, sliding mode control (Utkin et al., 2009) is selected here for the control problems of flexible joint robots. As it well known, sliding mode control theory can be applied to high-order, non-linear, uncertain MIMO systems and the resulting controllers are simple enough for practical implementations. Another advantage of sliding mode control

theory is easy to understand for normal control engineers (it is the main reason why this control theory becomes more and more popular). The major disadvantage associated with sliding mode control is the chattering phenomena due to the high frequency switching of the discontinuous control input. However, if the chattering problem can be solved or the inherent discontinuous property of the plant actuators (like electric motors) can be positively utilized, sliding mode control theory will be a good design tool for deriving the control algorithms. In this chapter, the design methodology of sliding mode control will be the major theoretical tool for the control of flexible joint robots.

The rest of this chapter is organized as follows:
In Section 2, the control problems for rigid-body robot manipulators with modelling uncertainties and external disturbances will be dealt with. The resulting control algorithm will be used for the link position tracking control of flexible joint robots. Section 3 handles the joint torque dynamics based on the singular perturbation approach. We use the result of other researchers without repeating the theory of singularly perturbed systems. Section 4 presents the theoretical derivation of sliding mode PWM for the current control of PMSM. This current controller will be used as the most internal control loop for the link position tracking control. Section 5 shows the simulation study, verifying the developed control algorithms, based on a dynamic model consisting of a two-link flexible joint robot with two joint motors. In section 6 some conclusions will be given.

2. Robust control of rigid manipulators based on integral sliding mode

2.1 Problem statement

For rigid body robot manipulators, the computed torque approach provides asymptotic stability for tracking control tasks. However, the state dependent matrices needed to complete the computed torque algorithm are normally unknown and possibly too complex for a real-time implementation. This section proposes a simple controller with computed-torque-like structure enhanced by integral sliding mode, having pole-placement capability. For the reduction of the chattering effect generated by the sliding mode part, the integral sliding mode is posed as a perturbation estimator with quasi-continuous control action provided by an additional low-pass filter. The time-constant of the latter tunes the controller functionality between the perturbation compensation and a pure integral sliding mode control, as well as between chattering reduction and system robustness.
Studies on the control of chain-like mechanical systems have been a subject of intensive and profitable research over the last three decades. Robot manipulators, as dynamically coupled non-linear MIMO systems have attracted the attention of many control scientists and engineers. Arbitrary assignment of the system poles of a set of decoupled and linearised sub-systems has been the final design goal. The computed torque (Hunt et al., 1983; Gilbert & Ha, 1984), as a theoretically simplest and most comprehensive approach for the tracking control of robot manipulators, allows one to assign the poles of the closed-loop system arbitrarily at the price of an exact feedback linearization with state dependent quantities for compensation of the system non-linearity with coupling terms. Any mismatch due to parameter or modelling uncertainties in the plant will violate exact linearization and decoupling. Moreover, even when these quantities are known exactly, the real-time

implementation is still an issue, since the computational overhead might be too large to prevent the control algorithm from being realized in control hardware.

Motivated by the recent developments on integral sliding mode control (Utkin & Shi, 1996; Poznyak et al., 2004; Cao & Xu, 2004; Castaños & Fridman, 2006; Utkin et al., 2009), by taking regard on algorithm complexity, this section proposes a novel control structure with pole-placement capability for rigid body robot manipulators. Simple matrices describing the nominal model (normally they are constant, as long as the available joint torques are high enough) are used to form a computed-torque-like controller, whereas two diagonal control gain matrices are responsible for the pole-placement. In addition, an additive control vector is designed based on the concept of integral sliding mode to compensate for the overall matched system uncertainties (for systems with unmatched uncertainties, other than the case of full actuated robot manipulators, the readers are referred to (Cao & Xu, 2004; Castaños & Fridman, 2006)).

Control of robot manipulators using sliding mode technique has a rather long history. Since the first set-point sliding mode controller suggested by (Young, 1978), numerous variations have been proposed in the literature, such as the component-wise control discussed by (Slotine, 1985) and by (Chen et al., 1990). The robustness property of the conventional sliding mode control with respect to variations of system parameters and external disturbances can only be achieved after the occurrence of sliding mode. During the reaching phase, however, there is no guarantee for robustness. Integral sliding mode aims at eliminating the reaching phase by enforcing the sliding mode on the entire system response (Utkin & Shi, 1996). As a result, robustness of the system can be guaranteed starting from the initial time instant, that is, a robot manipulator is able to track the reference trajectory (with designed error dynamics given by the pole placement) throughout the entire system response despite the system uncertainties.

However, since a discontinuous term appears in the resulting joint torque, direct implementation of the integral sliding mode control algorithm may be difficult due to the chattering effect. To solve this implementation problem i.e. to reduce the chattering level, the discontinuous term is used for a perturbation estimator based on an auxiliary internal dynamic process. It will be shown that the equivalent control of such a discontinuous term is indeed able to compensate the net system perturbation.

If the equivalent control could be obtained exactly, the system perturbation could be compensated for completely, so that the system would be free of chattering and robust starting from the initial time instant. Strictly speaking, the exact equivalent control based on the system model is impossible to achieve, primarily due to model uncertainties. However, if the spectrum of the equivalent control has no overlap with the switching frequency of the discontinuous control term (it is normally the case in practice), a low-pass filter can be used to extract the equivalent control from the discontinuous control term (Utkin, 1992). Using low-pass filter to extract equivalent control from the discontinuous control term provides the basic information source of proposed control design.

From the practical point of view, the bandwidth of the low-pass filter is designed as low as possible, so that the amplitude of the chattering remains low level. However, since the frequency of the equivalent control is time-varying, a low-pass filter with a fixed time-constant and low bandwidth would “cut” the equivalent control and lose the information about the system perturbation. Thus, there is a trade-off between the system robustness

(whether the system perturbation can be compensated for completely) and the chattering reduction by tuning of the time-constant of the low-pass filter.

2.2 Integral sliding mode control and perturbation estimator

In this section, the basic concept and the main result of integral sliding mode control will be outlined.

For a given dynamic system represented by the following state space equation

$$\dot{x} = f(x) + B(x)u + h(x,t) \tag{1}$$

with $x \in \Re^n$ being the state vector, $u \in \Re^m$ being the control input vector ($rank\ B(x) = m$) and $h(x,t)$ being the perturbation vector due to model uncertainties or external disturbances; $h(x,t)$ is bounded and assumed to fulfil the matching condition. The control low for system (1) is proposed as

$$u = u_0 + u_1 \tag{2}$$

where $u_0 \in \Re^m$ is responsible for the performance of the nominal system; $u_1 \in \Re^m$ is a discontinuous control action that rejects the perturbations by ensuring the sliding motion. The sliding manifold is defined as

$$\begin{gathered} s = s_0(x) + z\ , \\ \text{with} \\ s,\ s_0(x),\ z \in \Re^m \\ \dot{z} = -\frac{\partial s_0}{\partial x}\{f(x) + B(x)u_0(x)\} \\ z(0) = -s_0(x(0)) \end{gathered} \tag{3}$$

where initial condition $z(0)$ is determined under the requirement $s(0) = 0$. It can be proven that the equivalent control of u_1 will cancel out the perturbation term $h(x,t)$, see (Utkin et al. 2009). Discontinuous control u_1 has a proper selected control gain which ensures sliding motion starting from $t = 0$ i.e. $s(0) = 0$.

In real applications, however, discontinuous control u_1 may result in chattering effect, imposing high frequency vibrations. To reduce this undesired effect, the control system can be modified as follows:

$$\begin{gathered} s = s_0(x) + z \\ \dot{z} = -\frac{\partial s_0}{\partial x}\{f(x) + B(x)u - B(x)u_1\} \\ z(0) = -s_0(x(0)) \\ u = u_0 + u_{1av} \\ u_{1av} = lowpass(u_1) \end{gathered} \tag{4}$$

By solving equation $\dot{s}=0$ for u_1, it can be directly checked that the equivalent control of u_1 still cancels the system perturbation. In the above controller, relation $u_{1eq}=u_{1av}$ is used, for proof see (Utkin, 1992). Finally, the term u_{1av} is quasi-continuous (depending on the time-constant of the low-pass filter) and equal to the perturbation term to be compensated for, serving as the perturbation estimator. Moreover, since discontinuous control u_1 appears only in the control computer, its gain is more flexible to tune.

2.3 Control of robot manipulators

2.3.1 Model of rigid body robot manipulators

The model of a rigid body robot manipulator with n degrees of freedom can be written as

$$M(q)\ddot{q}+C(q,\dot{q})\dot{q}+G(q)+F(\dot{q})=\tau \tag{5}$$

where $M(q)\in\Re^{n\times n}$ is the mass matrix; $C(q,\dot{q})\dot{q}\in\Re^n$ is the vector including centrifugal and Coriolis forces; $G(q)\in\Re^n$ is the gravity force vector; $F(\dot{q})\in\Re^n$ is the friction force vector; $q\in\Re^n$ represents the joint position vector and $\tau\in\Re^n$ denotes the joint torque vector.
For the purpose of control design, the notation of the above model can be formally changed to

$$M(q)\ddot{q}+N(q,\dot{q})=\tau \tag{6}$$

where vector $N(q,\dot{q})=C(q,\dot{q})\dot{q}+G(q)+F(\dot{q})$ does not contain term $\ddot{q}$. This model can be rewritten as the sum of an ideal model and a perturbation term:

$$M_0(q)\ddot{q}+N_0(q,\dot{q})=\tau+H(q,\dot{q},\ddot{q}) \tag{7}$$

where $M_0(q)=M(q)-\Delta M$, $N_0(q,\dot{q})=N(q,\dot{q})-\Delta N$, with ΔM and ΔN being the unknown part of matrix $M(q)$ and vector $N(q,\dot{q})$, respectively; vector $H(q,\dot{q},\ddot{q})$ denotes the overall system perturbation and has the form $H(q,\dot{q},\ddot{q})=-(\Delta M\,\ddot{q}+\Delta N)$. Note that the perturbation term $H(q,\dot{q},\ddot{q})$ satisfies the matching condition.

2.3.2 Control design using integral sliding mode

Following the design principle given in section 2.2, the joint torque vector τ can be designed as two additive terms:

$$\begin{aligned}\tau&=\tau_0+\tau_1\\ \tau_0&=M_0(q)(\ddot{q}_d-K_D\dot{q}_e-K_Pq_e)+N_0(q,\dot{q})\end{aligned} \tag{8}$$

where $M_0(q)$, $N_0(q,\dot{q})$ are the nominal value of $M(q)$, $N(q,\dot{q})$, respectively, as defined with equation (7); $K_P\in\Re^{n\times n}$, $K_D\in\Re^{n\times n}$ are positive definite diagonal gain matrices

determining the closed loop performance; and the tracking error is defined as $q_e(t) = q(t) - q_d(t)$ with $\begin{bmatrix} q_d(t) & \dot{q}_d(t) & \ddot{q}_d(t) \end{bmatrix}$ being the reference trajectory and its time derivatives. Note that τ_0 represents the computed torque part of the controller.

Discontinuous control τ_1 is now derived based on the design principle of integral sliding model control:

Step 1: Sliding Manifold

The sliding manifold is defined based on equation (3)

$$\begin{aligned} s &= s_0(x) + z \\ s_0 &= \begin{bmatrix} C & I \end{bmatrix} \begin{bmatrix} q_e \\ \dot{q}_e \end{bmatrix} \\ \dot{z} &= -\begin{bmatrix} C & I \end{bmatrix} \begin{bmatrix} \dot{q}_e \\ -M_0^{-1}N_0 + M_0^{-1}\tau_0 - \ddot{q}_d \end{bmatrix} \\ z(0) &= -Cq_e(0) - \dot{q}_e(0) \end{aligned} \tag{9}$$

where $C \in \Re^{n \times n}$ is a positive definite gain matrix and $I \in \Re^{n \times n}$ is a $n \times n$ unit matrix.

Vector s can be further simplified by substituting τ_0 with equation (8):

$$s = \dot{q}_e + K_D q_e + K_P \int_0^t q_e(\xi) d\xi - \dot{q}_e(0) - K_D q_e(0) \tag{10}$$

Since the requirement $s(0) = 0$ is satisfied, sliding mode will occur starting from the initial time instant $t = 0$. Note that for the implementation of s, matrix C is not required in the final equation, see (10). As one can see from the derivations given above, equation (10) is the natural extension of the basic design equation of integral sliding mode (3).

To prepare the stability analysis, the time derivative of the sliding variable $s(t)$ can be obtained

$$\dot{s} = \dot{s}_0 + \dot{z} = \zeta_1 + \zeta_2 \tau_0 + M^{-1}\tau_1 \tag{11}$$

where $\zeta_1 = (M_0^{-1}N_0 - M^{-1}N)$ and $\zeta_2 = (M^{-1} - M_0^{-1})$ represent the mismatches between the nominal parameters $M_0(q)$, $N_0(q, \dot{q})$, and the real system parameters $M(q)$, $N(q, \dot{q})$, respectively, viewed as system perturbation terms. Note that in this study we assume that both ζ_1 and $\zeta_2 \tau_0$ are norm-bounded.

Step 2: Discontinuous control τ_1

τ_1 is the discontinuous control dedicated to reject the overall perturbation torque $H(q, \dot{q}, \ddot{q})$.

Here τ_1 can be selected as

$$\tau_1 = -\Gamma_0 \frac{s}{\|s\|} \tag{12}$$

where Γ_0 is a positive constant (control gain may also take other forms) and $\|s\|$ denotes the norm 2 of s i.e. $\|s\| = \sqrt{s_1^2 + s_2^2 + \cdots s_n^2}$.

Step 3: Design of the control gain Γ_0

Select a Lyapunov function candidate as $V = \frac{1}{2} s^T s > 0$ (for $s \neq 0$). The time derivative of V along the solutions of (11) is given by

$$\dot{V} = s^T \dot{s} = s^T (\zeta_1 + \zeta_2 \tau_0) - \Gamma_0 s^T M^{-1} s / \|s\| \tag{13}$$

Since matrix $M^{-1}(q)$ is positive definite and Γ_0 is a positive constant, the most right term in (13) i.e. $\Gamma_0 s^T M^{-1} s / \|s\|$ is positive for any $s \neq 0$. For a small enough positive number ρ, such that inequality $\Gamma_0 s^T M^{-1} s / \|s\| \geq \Gamma_0 s^T \rho s / \|s\|$ holds, it can be shown that

$$\dot{V} \leq -\|s\| \left(\Gamma_0 \rho - \|\zeta_1 + \zeta_2 \tau_0\| \right) \tag{14}$$

Clearly, under the norm-boundedness condition of terms ζ_1 and $\zeta_2 \tau_0$, a large enough gain Γ_0 can always be chosen to guarantee $\dot{V} < -\alpha \|s\|$ (with $\alpha > 0$ and for $\|s\| \neq 0$), implying the occurrence of sliding mode in finite time. Note that the initial conditions in (10) eliminate the reaching phase.

Step 4: Equivalent control of τ_1

Once sliding mode occurs and the system is confined to the manifold $s(t) = 0$, the equivalent control of τ_1 can be used to examine the system behaviour. The equivalent control is obtained by formally setting $\dot{s} = 0$, yielding

$$\tau_{1eq} = -M(\zeta_1 + \zeta_2 \tau_0) \tag{15}$$

Substitution of $\tau = \tau_0 + \tau_{1eq}$ in equation (6) with equivalent control (15) leads to the motion equation in sliding mode, which can be simplified as

$$M_0(q)\ddot{q} + N_0(q, \dot{q}) = \tau_0 \tag{16}$$

Control τ_0 in (8) thus achieves the designed (closed-loop) error dynamics defined by K_D and K_P, namely

$$\ddot{q}_e + K_D \dot{q}_e + K_P q_e = 0 \tag{17}$$

as if perturbation term $H(q,\dot{q},\ddot{q})$ in (7) would not have existed. Equation (16) as well as (17) represents the system motion in sliding mode. Solving $\ddot{q}$ from (16) and setting into $H(q,\dot{q},\ddot{q})$, easily shows the perturbation cancellation property, i.e. $\tau_{1eq} = -H(q,\dot{q},\ddot{q})$. The derivation above is only to show the perturbation cancellation property by the equivalent control τ_{1eq}. Actually, the designed closed loop motion presented by (17) can be obtained more easily by taking the time derivative of (10) and set $\dot{s} = 0$.
Summarization of the integral sliding mode control system for the implementation:

$$\begin{aligned} \tau_0 &= M_0(q)(\ddot{q}_d - K_D\dot{q}_e - K_P q_e) + N_0(q,\dot{q}) \\ s &= \dot{q}_e + K_D q_e + K_P \int_0^t q_e(\xi)d\xi - \dot{q}_e(0) - K_D q_e(0) \\ \tau_1 &= -\Gamma_0 \frac{s}{\|s\|} \\ \tau &= \tau_0 + \tau_1 \end{aligned} \tag{18}$$

From (18), one can see the benefit of the control system: in order to assign the poles of the closed-loop system arbitrarily, one needs only to additionally calculate the variable s and τ_1, exact knowledge about $M(q)$ and $N(q,\dot{q})$ are not required. Depending on the available control resource, the nominal quantities $M_0(q)$, $N_0(q,\dot{q})$ can even be set constant i.e. to M_0, N_0. Moreover, the robustness of the tracking control performance is ensured starting from $t = 0$.

2.3.3 Control design using integral sliding mode based perturbation estimator

Hitherto, the control system described in section 2.3.2 looks perfect. However, in some practical applications, the controller given in (18) may not be applicable to robot manipulators, as the chattering level generated by the discontinuous control term τ_1 may be very high. Following the control design approach given by (4), the control system can be modified to:

$$\begin{aligned} \tau_0 &= M_0(q)(\ddot{q}_d - K_D\dot{q}_e - K_P q_e) + N_0(q,\dot{q}) \\ s &= \dot{q}_e + K_D q_e + K_P \int_0^t q_e(\xi)d\xi - \dot{q}_e(0) - K_D q_e(0) + \int_0^t M_0^{-1}(q)(\tau_1 - \tau_{1av})d\xi \\ \tau_1 &= -\Gamma_0 \frac{s}{\|s\|} \\ \tau_{1av} &= lowpass(\tau_1) \\ \tau &= \tau_0 + \tau_{1av} \end{aligned} \tag{19}$$

Note that for a better decoupling, the control gain of τ_1 may also be selected as $M_0\Gamma_0$ instead of Γ_0. However, since we are intended to compare the solution based on the perturbation estimator with the pure integral sliding mode control (18), the control gain is designed to have the same form for the both control systems. Now, the equivalent control of τ_1 can be obtained by setting $\dot{s}=0$

$$\begin{aligned} \dot{s} &= \dot{s}_0 + \dot{z} = \zeta_1 + \zeta_2\tau + M_0^{-1}\tau_1 = 0 \\ \tau_{1eq} &= -M_0(\zeta_1 + \zeta_2\tau) \end{aligned} \tag{20}$$

Actually, since $\tau = \tau_0 + \tau_{1av} = \tau_0 + \tau_{1eq}$, (20) can be further simplified to (15), implying that the equivalent control τ_{1eq} remains the same as in the case of pure integral sliding mode control.

For the convergence proof of s to zero, check that the dynamic motion about s in the closed-loop system can be derived as

$$\dot{s} = \dot{s}_0 + \dot{z} = \zeta_1 + \zeta_2\tau - M_0^{-1}\tau_1 \tag{21}$$

For a Lyapunov function candidate $V = \frac{1}{2}s^T s > 0$ (for $s \neq 0$), the time derivative of V along the solutions of (21) can be obtained as

$$\dot{V} = s^T\dot{s} = s^T(\zeta_1 + \zeta_2\tau) - \Gamma_0 s^T M_0^{-1} s/\|s\| \tag{22}$$

Similar lines as in (14) can be followed to show that a large enough control gain Γ_0 can be selected such that $\dot{V} < -\alpha\|s\|$ (with $\alpha > 0$ and for $\|s\| \neq 0$), implying that sliding mode will be enforced in finite time. Note that τ in (22) is now quasi-continuous due to the low-pass filter, it can be assumed here that terms ζ_1 and $\zeta_2\tau$ are norm-bounded. Again, initial conditions guarantee that $s(0)=0$ in (19), thus eliminating the reaching phase.

The advantage of controller (19) over the previous controller given by (18) is: the discontinuous control term τ_1 (with gain Γ_0) appears only in the control computer and the real control τ applied to the robot manipulator (see (19)) is low-pass filtered. Control term τ_{1av} serves here as a perturbation compensator. As one can see from (19), if the time constant of the low-pass filter tends to zero, the controller given by (19) will converge to controller (18), i.e. from perturbation estimation solution to integral sliding mode control solution. For the control system under controller (19), sliding mode $s(t) \equiv 0$ is guaranteed throughout the entire system response, although a low-pass filter is involved in the control loop.

2.3.4 Practical consideration

Since low-order filters do not ideally cut off the high-frequency switching signal components due to the discontinuous term τ_1, some amount will be still preserved in τ_{1av}.

Whereas for practical applications, a large time constant for the low-pass filter is normally preferred, such that the resulting control signals remain as smooth as possible. However, since the instantaneous frequency of the system perturbation (i.e. the frequency of τ_{1eq} after sliding mode occurs) is unknown and time changing, it may happen that the bandwidth of τ_{1eq} is higher than the bandwidth of the low-pass filter and the system perturbation cannot be cancelled out completely, thus the system robustness is reduced. For a high control performance, the time constant of the low-pass filter should be made small (at least during the transient period) such that the bandwidth of the low-pass filter is high enough and τ_{1eq} can get through the filter completely.
As a result, in the practical implementation the time constant of the low-pass filter can be used as a trade-off between chattering reduction and system robustness: if a high robustness as well as high control accuracy during the transient period is required, the time constant of the low-pass filter can be made small for the short time period. The trade-off between chattering reduction and system robustness by changing the time constant of the low-pass filter is demonstrated in Sections 5.2 and 5.3.

3. Singular perturbation approach to handle the joint flexibility

As mentioned in the introduction part, singular perturbation approach has at least the following advantages:
(a). the signals for the control implementation can be made available
(b). there is no need to implement an exact tracking controller for the joint torque
(c). the results for the control of rigid-body robots can be used further
(d). the implementation of the control algorithm is easy

Sure, singular perturbation approach has also disadvantages:
(a). it is not valid if the joint stiffness is too low
(b). the control law is sensitive to the change of joint stiffness
Fortunately, most of lightweight manipulators used in practice have high enough and fixed joint stiffness. The flexibility in robot joints is a side-effect to achieve lightweight and it is normally not intended by the robot designer.
The control algorithm of this section will be summarized here without repeating the theory of singularly perturbed systems. The way of treating the joint torque dynamics can be find e.g. in (Ott, 2008).
The output of the robust link position controller for rigid body manipulators given in Section 2 is denoted here as τ_d (instead of τ), which is the reference input for the joint torque implementation. Normally, when using singular perturbation approach for the control of slow dynamics, the joint inertia matrix J has to be considered in the link position controller by adding matrix J to the mass-matrix of the robot arm $M(q)$. However, since our link position controller is a robust controller, implying that no exact parameters are required, the information about the joint inertia is normally not necessary (the system robustness depends on the available control resource).

The reference current vector for the joint motors can be calculated from the slow and fast torque components i.e. $\tau_s \in R^n$ and $\tau_f \in R^n$ for stabilizing the joint torque dynamics

$$I_q^* = K_t^{-1}\tau_m = K_t^{-1}G_r^{-1}(\tau_s + \tau_f) \tag{23}$$

where K_t is the diagonal torque constant matrix of the electric motors and G_r is the diagonal gear-ratio matrix; $I_q^* = [i_{qi}^*] \in R^n$, with $i = 1 \sim n$, is the reference current vector including the reference currents for all joints; τ_m represents the motor torque vector. The slow and fast joint torque components can be given as

$$\begin{gathered} \tau_s = \tau_d \\ \tau_f = -D_\tau \dot{\tau} \\ \text{or} \\ \tau_f = -K_\tau(\tau - \tau_d) - D_\tau \dot{\tau} \end{gathered} \tag{24}$$

with $D_\tau \in R^{n\times n}$ and $K_\tau \in R^{n\times n}$ being constant diagonal control gain matrices to be determined by the control designer (if the joint stiffness is changed the control gain matrices need to be retuned accordingly).

4. Direct current control using sliding mode PWM

When using the build-in PWM unit of a micro-controller or a DSP, the required reference voltage signals generated by the current controller will be modulated in form of pulse-width and then it is hoped that the average value of the terminal voltages of the stator windings will be equal to the reference voltages that the current controller produces. In this configuration there are two problems:
(a). the PWM implementation of the terminal voltages is done in a way of open-loop, the final voltages on the stator windings may differ from the ones what current controller requires, depending on the quality of the pulse-width-modulation.
(b). it introduces some time delay, at lease a duty-cycle has to remain unchanged before the corresponding PWM signal being sent out.
Thus for a high dynamic performance, the build-in PWM unit of a micro-controller or a DSP has some disadvantages.
On the other hand, the conventional current control hardware such as Chopper-Control or Hysteresis-Control hardware do not have these disadvantages. Because no micro-processor being available, these practically used hardware were not able to implement the concept of field-oriented control. In this section we derive a current controller based on sliding mode control theory for PMSM which has the performance of field-oriented control, but without the disadvantage associated with the open-loop PWM techniques. We call this kind of current control "sliding mode PWM current control".
At first, we need the motor model to design the current controller. The motor model in the (d, q)-coordinate frame, which rotates synchronously with the motor rotor, can be given as

$$L\frac{di_d}{dt} = u_d - Ri_d + L\omega_e i_q$$
$$L\frac{di_q}{dt} = u_q - Ri_q - L\omega_e i_d - \lambda_0\omega_e \tag{25}$$

where L is the stator inductance and R is the stator resistance; i_d and i_q are the stator currents in the (d,q) coordinate frame; u_d and u_q are the stator voltages in the same coordinate frame; λ_0 is the flux constant of the rotor permanent magnet; ω_e is the rotor electric angular speed.

For the sliding mode current controller, the switching functions for the d and q current components are designed as

$$s_d = i_d - i_d^*$$
$$s_q = i_q - i_q^* \tag{26}$$

where i_q^* is the reference current i.e. one of the components of the compose controller (23) (index i is neglected here for simplicity), and reference current component $i_d^* = 0$ for constant torque operation and $i_d^* \neq 0$ for field-weakening operation (Shi & Lu, 1996). The time derivative of both switching functions along the solutions of (25) can be found as

$$\dot{s}_d = \dot{i}_d - \dot{i}_d^* = \frac{1}{L}u_d - \frac{R}{L}i_d + \omega_e i_q - \dot{i}_d^*$$
$$\dot{s}_q = \dot{i}_q - \dot{i}_q^* = \frac{1}{L}u_q - \frac{R}{L}i_q - \omega_e i_d - \frac{\lambda_0}{L}\omega_e - \dot{i}_q^* \tag{27}$$

Introducing two auxiliary variables f_d and f_q as follows

$$f_d = -\frac{R}{L}i_d + \omega_e i_q - \dot{i}_d^*$$
$$f_q = -\frac{R}{L}i_q - \omega_e i_d - \frac{\lambda_0}{L}\omega_e - \dot{i}_q^* \tag{28}$$

(27) will be simplified to

$$\dot{s}_d = f_d + L^{-1}u_d$$
$$\dot{s}_q = f_q + L^{-1}u_q \tag{29}$$

The above equation system can be summarized in vector form, resulting in

$$\begin{bmatrix} \dot{s}_d \\ \dot{s}_q \end{bmatrix} = \begin{bmatrix} f_d \\ f_q \end{bmatrix} + L^{-1} \begin{bmatrix} u_d \\ u_q \end{bmatrix} \tag{30}$$

Here stator voltages u_d and u_q are not yet the discontinuous voltages applied to the stator windings. For the sliding mode current control we need the relationship between the final discontinuous voltages applied to the stator windings i.e. $u_1 \sim u_3$ (which take the values from the set $\{-u_0, u_0\}$ with u_0 being the DC-Bus voltage) and the time derivative of both switching functions. This relationship can be given as

$$\begin{bmatrix} \dot{s}_d \\ \dot{s}_q \end{bmatrix} = \begin{bmatrix} f_d \\ f_q \end{bmatrix} + L^{-1} \begin{bmatrix} u_d \\ u_q \end{bmatrix} = \begin{bmatrix} f_d \\ f_q \end{bmatrix} + L^{-1} A_{d,q}^{1,2,3} \begin{bmatrix} u_1 \\ u_2 \\ u_3 \end{bmatrix} \tag{31}$$

where matrix $A_{d,q}^{1,2,3}$ can be expended as

$$A_{d,q}^{1,2,3} = \begin{bmatrix} \cos\theta_a & \cos\theta_b & \cos\theta_c \\ -\sin\theta_a & -\sin\theta_b & -\sin\theta_c \end{bmatrix} \tag{32}$$

with $\theta_a = \theta_e$, $\theta_b = \theta_e - 2\pi/3$, $\theta_c = \theta_e + 2\pi/3$ and θ_e being the rotor electrical angular position. Using (32), (31) can be rewritten as

$$\begin{bmatrix} \dot{s}_d \\ \dot{s}_q \end{bmatrix} = \begin{bmatrix} f_d \\ f_q \end{bmatrix} + L^{-1} \begin{bmatrix} u_1 \cos\theta_a + u_2 \cos\theta_b + u_3 \cos\theta_c \\ -u_1 \sin\theta_a - u_2 \sin\theta_b - u_3 \sin\theta_c \end{bmatrix} \tag{33}$$

To find the control signals u_1, u_2 and u_3, Lyapunov approach can be employed. Design a Lyapunov function candidate as

$$V = \frac{1}{2} \boldsymbol{S}_{dq}^T \boldsymbol{S}_{dq} \tag{34}$$

where $\boldsymbol{S}_{dq} = [s_d \;\; s_q]^T$. The time derivative of V along the solution of (33) can be found as

$$\begin{aligned} \dot{V} &= \boldsymbol{S}_{dq}^T \dot{\boldsymbol{S}}_{dq} \\ &= \begin{bmatrix} s_d & s_q \end{bmatrix} \begin{bmatrix} \dot{s}_d \\ \dot{s}_q \end{bmatrix} \\ &= \begin{bmatrix} s_d & s_q \end{bmatrix} \begin{bmatrix} f_d \\ f_q \end{bmatrix} + L^{-1} \begin{bmatrix} s_d & s_q \end{bmatrix} \begin{bmatrix} u_1 \cos\theta_a + u_2 \cos\theta_b + u_3 \cos\theta_c \\ -u_1 \sin\theta_a - u_2 \sin\theta_b - u_3 \sin\theta_c \end{bmatrix} \end{aligned} \tag{35}$$

which can be further expanded to

$$\begin{aligned}\dot{V} &= \boldsymbol{S}_{dq}^{T}\dot{\boldsymbol{S}}_{dq} \\ &= (s_d f_d + s_q f_q) + L^{-1}[u_1(s_d\cos\theta_a - s_q\sin\theta_a) + u_2(s_d\cos\theta_b - s_q\sin\theta_b) + u_3(s_d\cos\theta_c - s_q\sin\theta_c)]\end{aligned} \tag{36}$$

Introducing the following three auxiliary variables

$$\begin{aligned}\Omega_1 &= (s_d\cos\theta_a - s_q\sin\theta_a) \\ \Omega_2 &= (s_d\cos\theta_b - s_q\sin\theta_b) \\ \Omega_3 &= (s_d\cos\theta_c - s_q\sin\theta_c)\end{aligned} \tag{37}$$

equation (36) can be simplified to

$$\dot{V} = (s_d f_d + s_q f_q) + L^{-1}(u_1\Omega_1 + u_2\Omega_2 + u_3\Omega_3) \tag{38}$$

In order to guarantee $\dot{V} < 0$, the control signals u_1, u_2 and u_3 can be designed as

$$\begin{aligned}u_1 &= -u_0 sign(\Omega_1) \\ u_2 &= -u_0 sign(\Omega_2) \\ u_3 &= -u_0 sign(\Omega_3)\end{aligned} \tag{39}$$

With these notations, equation (38) can be reformulated for the final analysis

$$\begin{aligned}\dot{V} &= (s_d f_d + s_q f_q) - L^{-1}u_0[sign(\Omega_1)\Omega_1 + sign(\Omega_2)\Omega_2 + sign(\Omega_3)\Omega_3] \\ &= (s_d f_d + s_q f_q) - L^{-1}u_0[|\Omega_1| + |\Omega_2| + |\Omega_3|]\end{aligned} \tag{40}$$

In the above equation, L^{-1} is a constant (but may be unknown). If the scalar term $(s_d f_d + s_q f_q)$ is bounded and if the DC-bus voltage u_0 is high enough, $\dot{V} < 0$ can be guaranteed, implying that the real currents will converge to their reference counterparts in finite time. Thus the stability of the current control system can be ensured under two conditions

(a). the DC-bus voltage u_0 is high enough

(b). auxiliary variables f_d and f_q are bounded

Since f_d and f_q do not contain the control voltages, neither u_d and u_q, nor u_1, u_2 and u_3, the condition (b) is reasonable. Note that if the reference currents i_d^* and i_q^* change too fast, the stability condition may be violated from time to time (depending on the available DC-bus voltage u_0). In this case there exists no current controller which can do better. Some researchers design sliding mode link position controller with discontinuous joint torque commands and without taking into account the motor dynamics, would meet this problem. Other high gain link position controllers without taking into account the motor dynamics would meet the same problem.

Now the implementation procedure is summarized.

Though the derivation of the proposed current controller looks rather involved, the implementation of this controller is quite simple. The equations for the implementation are summarized as follows

$$\begin{aligned} s_d &= i_d - i_d^* \\ s_q &= i_q - i_q^* \end{aligned}, \quad \begin{aligned} \Omega_1 &= (s_d \cos\theta_a - s_q \sin\theta_a) \\ \Omega_2 &= (s_d \cos\theta_b - s_q \sin\theta_b) \\ \Omega_3 &= (s_d \cos\theta_c - s_q \sin\theta_c) \end{aligned}, \quad \begin{aligned} u_1 &= -u_0 sign(\Omega_1) \\ u_2 &= -u_0 sign(\Omega_2) \\ u_3 &= -u_0 sign(\Omega_3) \end{aligned} \tag{41}$$

with $\theta_a = \theta_e$, $\theta_b = \theta_e - 2\pi/3$, $\theta_c = \theta_e + 2\pi/3$. The final gating signals taking values from set {0, 1} (like PWM signals) feeding to the inverter can be found as

$$\begin{aligned} s_{w1} &= 0.5\left(1 + u_1/u_0\right), \\ s_{w4} &= 1 - s_{w1}, \\ s_{w2} &= 0.5\left(1 + u_2/u_0\right), \\ s_{w5} &= 1 - s_{w2}, \\ s_{w3} &= 0.5\left(1 + u_3/u_0\right), \\ s_{w6} &= 1 - s_{w3}. \end{aligned} \tag{42}$$

The switching control signals $s_{w1} \sim s_{w6}$ are pulse signals, the pulse width is not calculated from some duty-cycle, but determined directly and instantaneously by the current control errors in the field-oriented coordinates. Note that in practical implementation, several μs time delay is required between signal pair s_{wi} and s_{wi+3} ($i = 1 \sim 3$). This current control system does not require the motor parameters as well as the decoupling process, thus it is a robust current control system.

5. Simulation Studies

5.1 A two-link robot manipulator as an example

A planar, two-link manipulator with revolute joints, taken from the example in (Utkin et al., 2009), is used here to demonstrate the proposed control approaches. The manipulator and the associated variables are depicted in Figure 1.

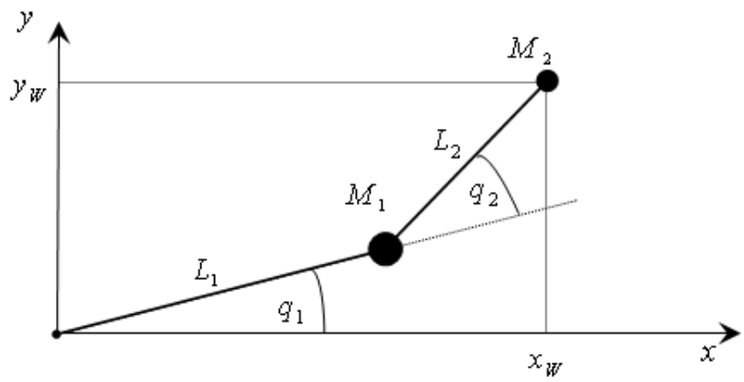

Fig. 1. Two-link manipulator with link lengths L_1 and L_2, and concentrated link masses M_1 and M_2. The manipulator is shown in joint configuration (q_1, q_2), which leads to end-effector position (x_W, y_W) in world coordinates.

The end-effector position, (x_W, y_W), i.e. the location of mass M_2 in world coordinate frame (x, y), is given by

$$\begin{aligned} x_W &= L_1 \cos q_1 + L_2 \cos(q_1 + q_2), \\ y_W &= L_1 \sin q_1 + L_2 \sin(q_1 + q_2), \end{aligned} \tag{43}$$

where (q_1, q_2) denotes the joint displacements and L_1, L_2 are the link lengths. Solving (43) for the joint displacements as a function of the end-effector position (x_W, y_W) yields the inverse kinematics as

$$\begin{aligned} q_2 &= \operatorname{atan2}(D, C), \quad \text{with} \quad C = \frac{x_W^2 + y_W^2 - L_1^2 - L_2^2}{2L_1 L_2}, \; D = \pm\sqrt{1 - C^2} \\ q_1 &= \operatorname{atan2}(y_W, x_W) - \operatorname{atan2}(L_2 \sin q_2, L_1 + L_2 \cos q_2) \end{aligned} \tag{44}$$

which obviously is not unique due to the two sign options of the square root in variable D. The function "atan2(.)" describes the arctan function normalized to the range $\pm 180^\circ$.
The dynamic model of the two-link manipulator can be given as

$$\begin{aligned} &\begin{bmatrix} m_{11} & m_{12} \\ m_{21} & m_{22} \end{bmatrix} \begin{bmatrix} \ddot{q}_1 \\ \ddot{q}_2 \end{bmatrix} + \begin{bmatrix} c_1 + g_1 + f_1 \\ c_2 + g_2 + f_2 \end{bmatrix} = \begin{bmatrix} \tau_1 \\ \tau_2 \end{bmatrix}, \text{i.e.} \\ &M(q) = \begin{bmatrix} m_{11} & m_{12} \\ m_{21} & m_{22} \end{bmatrix}, \; N(q, \dot{q}) = \begin{bmatrix} c_1 + g_1 + f_1 \\ c_2 + g_2 + f_2 \end{bmatrix}, \end{aligned} \tag{45}$$

with

$$
\begin{aligned}
&m_{22} = L_2^2 M_2, \\
&m_{12} = m_{21} = m_{22} + L_1 L_2 M_2 \cos q_2, \\
&m_{11} = L_1^2 (M_1 + M_2) + 2m_{12} - m_{22}, \\
&c_1 = -L_1 L_2 M_2 (2\dot{q}_1 \dot{q}_2 - \dot{q}_2^2) \sin q_2, \\
&c_2 = L_1 L_2 M_2 \dot{q}_1^2 \sin q_2, \\
&g_2 = L_2 M_2 g \cos(q_1 + q_2), \\
&g_1 = L_1 (M_1 + M_2) g \cos(q_1) + g_2, \\
&f_1 = k_{v1} \dot{q}_1 + k_{c1} sign(\dot{q}_1), \\
&f_2 = k_{v2} \dot{q}_2 + k_{c2} sign(\dot{q}_2),
\end{aligned}
\tag{46}
$$

where k_{vi} and k_{ci} ($i = 1,2$) are coefficients of viscous friction and coulomb friction, respectively.

The joint model for the two robot joints is given by

$$
\begin{aligned}
&J_i \ddot{\theta}_i + \tau_{dsi} + \tau_i = g_{ri} \tau_{mi} \\
&\tau_i = K_i (\theta_i - q_i) \quad i = 1 \sim 2
\end{aligned}
\tag{47}
$$

where the parameters and variables for the i^{th} joints are

q_i : link position
θ_i : joint position
τ_i : joint torque
τ_{mi} : motor torque
τ_{dsi} : disturbance torque
J_i : joint inertia
K_i : joint stiffness
g_{ri} : gear ratio

The electric motor model for each joint is taken from equation (25) with the transformation matrix given in (32).

The plant parameters for the simulation study are selected as shown in Table 1 through Table 3. Note that for the simulation, we select the joint disturbance torque in equation (47) as pure viscous friction $\tau_{dsi} = k_{\omega i} \dot{\theta}_i$ for both joints (but at link side both viscous and coulomb frictions are applied, see equation (46) and section 5.2).

M_1	M_2	L_1	L_2
2 kg	1 kg	0.5 m	0.5 m

Table 1. Arm Parameters

L (H)	R (Ohm)	λ_0 (Wb)	P	K_t (Nm/A)	$I_{q\_\max}$ (A)	u_0 (V)
22.5×10^{-3}	0.78	0.26	4	$(3/2)P\lambda_0$	50	100

Table 2. Parameters for motor 1 and motor 2 (P = number of pole-pair)

J (Kgm^2)	K (Nm/Rad)	g_r	k_ω (Nm/(Rad/s))
1.0	12000	20	1

Table 3. Parameters of joint 1 and joint 2

For the trajectory tracking control task, we will demand the manipulator to follow a circular trajectory in its workspace. The circle with centre (x_{d0}, y_{d0}) and radius r_d is given in world coordinates by

$$\begin{aligned} x_d(t) &= x_{d_0} + r_d\cos\psi_d \\ y_d(t) &= y_{d_0} - r_d\sin\psi_d \\ \psi_d(t) &= \frac{2\pi}{t_f}t - \sin\left(\frac{2\pi}{t_f}t\right),\ \ 0\le t\le t_f, \end{aligned} \tag{48}$$

where the operation is assumed to start at time $t=0$ and to be completed at final time $t=t_f$. Through the inverse kinematics, the reference link angles for joint 1 and joint 2 are calculated according to (44). The parameters for the reference trajectory are chosen as shown in Table 4.

x_{d0}	y_{d0}	r_d	t_f
0.25 m	0.25 m	0.5 m	2 s

Table 4. Parameters of reference circular trajectory.

5.2 Controller parameters and simulation configuration

The parameters for the outer link position control loop are selected as:

$$\begin{aligned} M_0(q) &= \begin{bmatrix} 2.5 & 0 \\ 0 & 1 \end{bmatrix}, \\ N_0(q,\dot{q}) &= \begin{bmatrix} 0 \\ 0 \end{bmatrix}, \\ K_p = \begin{bmatrix} 100 & 0 \\ 0 & 100 \end{bmatrix},\ K_d &= \begin{bmatrix} 20 & 0 \\ 0 & 20 \end{bmatrix}, \\ \Gamma_0 &= \begin{bmatrix} 400 & 0 \\ 0 & 400 \end{bmatrix} \end{aligned} \tag{49}$$

The joint torques of both joints are limited to 400Nm. To extract the equivalent control from the discontinuous control term to obtain $\tau_{1av} = \tau_{1eq}$ in equation (19), a simple first order low-pass filter is used i.e.

$$\mu \dot{y} = -y + u \tag{50}$$

where μ is the filter time-constant. In the simulation $\mu = 0.025$ is selected. In the transition period the frequency of τ_{1eq} may be higher than the edge-frequency of the low-pass filter, see the discussion in Section 2.3.4. To solve this problem, the time constant of the low-pass filter is made time varying:

$$\mu(t) = \begin{cases} (0.025/0.5)t, & 0 \le t \le 0.5 \\ 0.025, & t > 0.5 \end{cases} \tag{51}$$

Now the time constant of the low-pass filter is linearly increased from zero to 0.025s in half second and remains constant thereafter.

For the singular perturbation approach described in Section 3, the simple form $\tau_f = -D_\tau \dot{\tau}$ is used for the fast dynamics, where matrix D_τ is selected as

$$D_\tau = \begin{bmatrix} 0.001 & 0 \\ 0 & 0.001 \end{bmatrix} \tag{52}$$

Besides the large parameter mismatches between the values in the plant model and the nominal values used in the controller given by equation (49), some disturbances are added to the plant model to test the robustness of proposed control algorithms:

(a). the coefficients of viscous friction and coulomb friction in equation (46) are set as $k_{v1} = k_{v2} = 10Nm/(rad/s)$ and $k_{c1} = k_{c2} = 5Nm$, respectively. The generated friction terms are sufficient large with respect to gravitation forces, centrifugal and Coriolis forces in the plant model.

(b). an additional disturbance torque during 0 ~ 0.15s with constant amplitude of $-100Nm$ is added to both robot joints to test the robustness of the control system in the transition period.

5.3. Simulation results and discussion

The simulation results of the trajectory tracking controller for rigid-body robots presented in Section 2 have been given in (Shi et al., 2008), where different sliding mode control approaches under different system uncertainties are compared. In this section, we discuss only the simulation results for flexible joint robots, which are illustrated by Figure 2 through Figure 5.

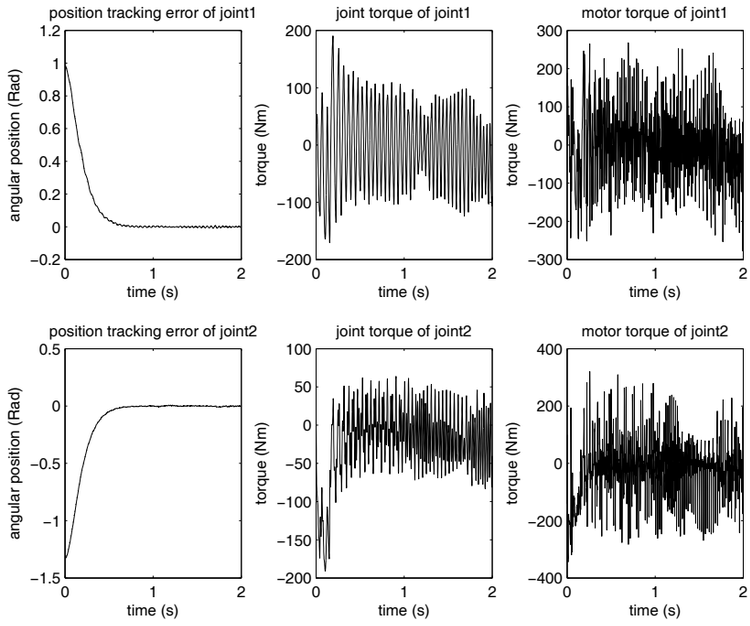

Fig. 2. Pure integral sliding mode control. Left plots: designed and real error dynamics of the link position tracking control (dotted-line: designed, solid-line: real, they are too close to be distinguished); middle plots: joint torque; right plots: required motor torque.

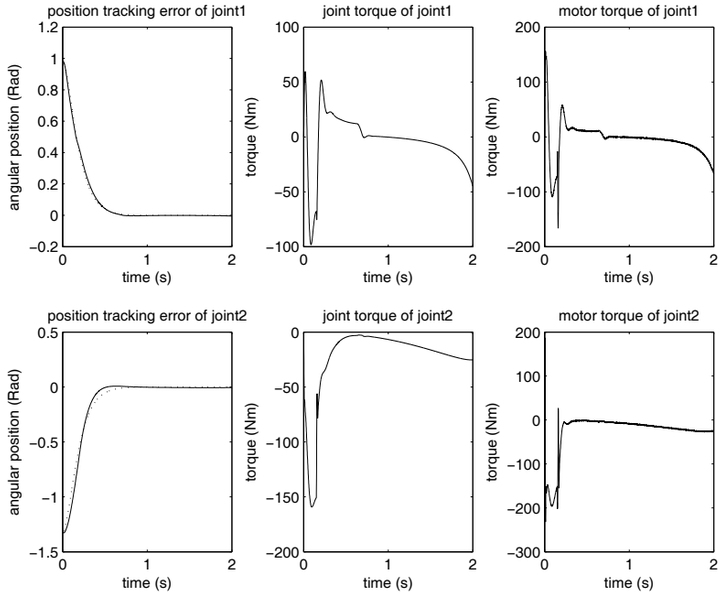

Fig. 3. Integral sliding mode based perturbation estimation approach with constant low-pass filter to extract the equivalent control. Left plots: designed and real error dynamics of the link position tracking control (dotted-line: designed, solid-line: real); middle plots: joint torque; right plots: required motor torque.

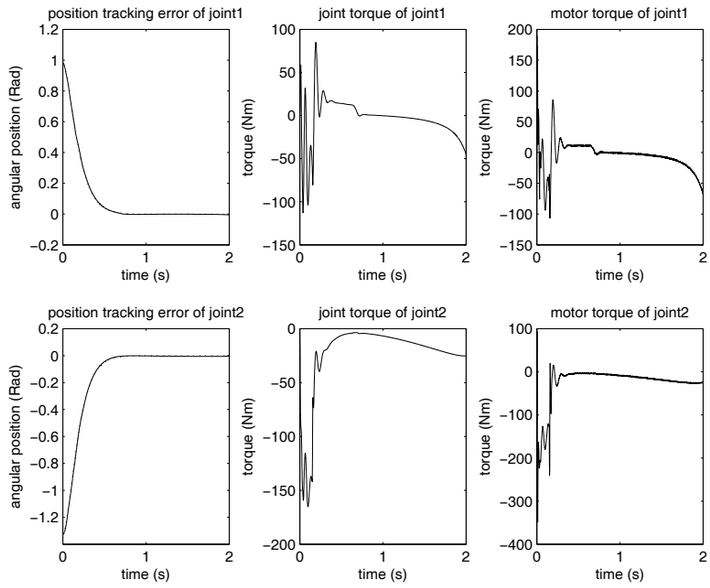

Fig. 4. Integral sliding mode based perturbation estimation approach with time varying low-pass filter to extract the equivalent control. Left plots: designed and real error dynamics of the link position tracking control (dotted-line: designed, solid-line: real, they are too close to be distinguished); middle plots: joint torque; right plots: required motor torque.

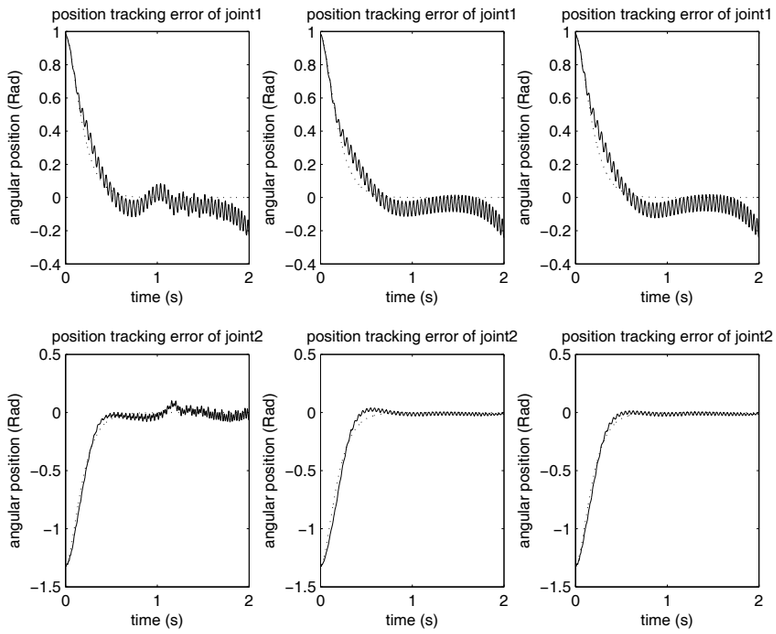

Fig. 5. Designed and real error dynamics of the link position tracking control (dotted-line: designed, solid-line: real) of the three control approaches, but without the singular perturbation treatment on the joint flexibility. Left plots: pure integral sliding mode control; middle plots: perturbation estimation approach with constant low-pass filter; right plots: perturbation estimation approach with time varying low-pass filter.

With Figure 2 the pure integral sliding mode control approach i.e. the controller given by equation (18) is demonstrated. For rigid-body robots, this controller has a prefect tracking control performance despite the large torque disturbance during the transition period (see (Shi et al., 2008)), but for flexible joint robots, the steady-state responses are not smooth enough, see both left plots in Figure 2. Similar to the case of rigid-body robots, there are high frequency oscillations in the joint torque and in the motor torque. The oscillation frequency for flexible joint robots is lower than the one for rigid-body robots because of the joint flexibility. For both types of robots this controller can not be used in practice due to the high level of chattering.

In Figure 3, the simulation result of the controller given by equation (19) is presented, where the low-pass filter is the first order linear filter given by equation (50) with constant μ. As one can see from the middle and right plots of figure, the joint torque and the required motor torques are smoothed significantly due to the perturbation estimation solution (implying that this controller can be applied to real world robot systems). However, the performance of the position tracking control is decreased a little bit, see the both left plots of the figure.

To recover the tracking control performance while keeping the joint torques and motor torques as smooth as possible, the time constant of the low-pass filter is made time varying according to equation (51). The simulation result is illustrated in Figure 4. Now, the position tracking control has a higher control accuracy, in both transition period and steady-state, see the both left plots of Figure 4. From the middle and right plots of Figure 4, one can see that the joint torques and the motor torques are still smooth enough, only in the transition period the frequency of these signals is higher than the case of Figure 3, because of the smaller time constant of the low-pass filter in this time range. Therefore, by tuning the time constant of the low-pass filter, the overall system performance can be improved.

The control approaches demonstrated by the simulation results given by Figure 2 through Figure 4 are supported by the singular perturbation treatment on the joint flexibility. Without this treatment, none of the control approaches can work properly, see Figure 5 (where all elements of matrix D_τ are set to zero). Therefore, joint torque signal as well as its time derivative is very important for the control of flexible joint robots.

6. Conclusion

The robust position tracking controller based on integral sliding mode for rigid-body manipulators is extended to the position tracking control of lightweight manipulators as well as flexible joint robots. Moreover, the control system takes the dynamics of joint motors into account. The joint flexibility is solved by singular perturbation approach which needs no parameter from the controlled system. Also, the current controller for the joint motors is a robust controller without involving the parameters of the electric motors and decoupling process. By using sliding mode PWM technique the current controller overcomes the disadvantages associated with the conventional build-in PWM in micro-processors or DSPs. For the link position tracking control only some rough nominal values are required. It is possible to achieve the pole-placement design without the exact knowledge about the manipulator system to be controlled. Moreover, the control design is mathematically easy and straightforward without involving the properties of the robot dynamics. The resulting control algorithms are simple enough for real-time implementation. The tradeoff between

chattering reduction and system robustness can be adjusted by the time constant of a low-pass filter. As the chattering level being significantly reduced, the control algorithms are applicable to real-life systems. Comparative simulation studies have confirmed the effectiveness of proposed control approaches and showed the potential toward the control of lightweight manipulators for high performance applications. Moreover, the presented design methodology can also be applied to other non-linear multi-variable dynamic systems.

7. References

Albu-Schaeffer, A. & Hirzinger, G. (2000). State feedback controller for flexible joint robots: a globally stable approach implemented on DLR's lightweight robots, *IEEE International Conference on Intelligent Robotic Systems*, pp. 1087-1093, ISBN: 0-7803-6348-5, Takamatsu, Japan, 2000

Albu-Schaeffer, A. (2002). Regelung von Robotern mit elastischen Gelenken am Beispiel der DLR-Leichtbauarme, PhD Thesis of TU Munich, 2002

Arimoto, S. (1994). State-of-the-art and future research direction of robot control, *Proceedings of 4th IFAC Symposium on Robot Control*, pp. 3-14, Capri, Italy, Sept. 1994

Cao, W. & Xu, J. (2004). Nonlinear integral-type sliding mode surface for both matched and unmatched uncertain systems, *IEEE Trans. Autom. Control*, Vol. 49, No. 8, Aug. 2004, pp. 1355–1360, ISSN : 0018-9286

Castaños, F. & Fridman, L. (2006). Analysis and design of integral sliding manifolds for systems with unmatched perturbations, *IEEE Transaction on Automatic Control*, Vol.51, No.5, 2006, pp.853-858, ISSN : 0018-9286

Chen, Y.-F.; Mita, T. & Wakui, S. (1990). A new and simple algorithm for sliding mode control of robot arms, *IEEE Trans. on Automatic Control*, Vol. 35, No. 7, 1990, pp. 828-829, ISSN: 0018-9286

De Luca, A. & Lucibello, P. (1998). A general algorithm for dynamic feedback linearization of robots with elastic joints, *IEEE International Conference of Robotics and Automation*, pp. 504-510, ISBN: 0-7803-4300-X, Leuven, Belgium, May 1998

Gilbert, E. & Ha, I. (1983). An approach to nonlinear feedback control with applications to Robotics, *IEEE Trans. on Systems, Man, and Cybernetics*, Vol. 22, Dec.1983, pp. 134-138

Gombert , B.; Hirzinger, G.; Plank, G.; Schedl, M. & Shi, J. (1995). Modular concepts for the new generation of DLR's light weight robots, *Proc. Third Conference on Mechatronics and Robotics*, pp. 30-43, 1995

Hirzinger, G.; Gombert, B.; Dietrich, J. & Shi, J. (1994). Transferring space robot technologies into terrestrial applications, *Proceedings of 25th International Symposium on Industrial Robots*, 1994

Hirzinger, G. ; Albu-Schaeffer, A. ; Haehnle, M. ; Schaefer, I. & Sporer, N. (2001). On a new generation of torque controlled light-weight robots, *IEEE International Conference of Robotics and Automation*, Vol. 4, 2001, pp. 3356-3363, ISSN: 1050-4729

Hirzinger, G.; Butterfass, J.; Grebenstein, M.; Haehnle, M.; Schaeferund, I. & Sporer, N. (2001). Space robotics-driver for a new mechatronic generation of lightweight arms and multi-fingered hands, *AIM*, Vol. 2, pp. 1160-1168, ISBN: 0-7803-6736-7, 2001, Como, Italy

Hunt, L.; Su, R. & Meyer, G. (1983). Global transformation of nonlinear systems, *IEEE Trans. on Automatic Control*, Vol. 28, No. 1, 1983, pp. 24-31, ISSN: 0018-9286

Koeppe, R. & Hirzinger, G. (2001). From human arms to a new generation of manipulators: control and design principles, *ASME Int. Mechanical Engineering Congress*, 2001

Lin, T. & Goldenberg, A.A. (1995). Robust adaptive control of flexible joint robots with joint torque feedback, *IEEE International Conference of Robotics and Automation*, Vol. 1, No. 4, May. 1995, pp. 1229-1234, ISSN: 1050-4729

Marino, R. & Spong, M. (1986). Nonlinear control techniques for flexible joint manipulators: a single link case study, *IEEE International Conference of Robotics and Automation*, Vol. 3, Apr. 1986, pp. 1030-1036

Ott, C. (2008). *Cartesian impedance control of redundant and flexible-joint robots,* Springer

Ozgoli, S. & Taghirad, H. D. (2006). A survey on the control of flexible joint robots, *Asian Journal of Control*, Vol. 8, No. 4, pp. 332-344, December 2006

Poznyak, A.; Fridman, L. & Bejarano, F. J. (2004). Mini-max integral sliding mode control for multimodel linear uncertain systems, *IEEE Trans. Autom. Control*, Vol. 49, No. 1, Jan. 2004, pp. 97–102, ISSN: 0191-2216

Readman, Mark C. (1994). *Flexible Joint Robots*, CRC Press

Slotine, J.-J.-E. (1985). The robust control of robot manipulators, *Int. Journal of Robotics Research*, No. 4, 1985, pp. 49-64

Slotine, J.-J.-E. & Li, W. (1987). On the adaptive control of robot manipulators, *Int. Journal of Robotics Research*, No. 6, 1987, pp. 49-59, ISSN:0278-3649

Schmidt, G. (2000). Lecture note: Grundlagen intelligenter roboter, TU München, Lehrstuhl fuer Steuerungs- und Regelungstechnik

Shi, J. & Lu, Y.S. (1996). Field-weakening operation of cylindrical permanent-magnet motors, *IEEE International Conference on Control Applications*, pp. 864-869, ISBN: 0-7803-2975-9, Dearborn, MI, USA, September 1996

Shi, J.; Albu-Schaeffer, A. & Hirzinger, G. (1998). Key issues in dynamic control of lightweight robots for space and terrestrial applications, *IEEE International Conference of Robotics and Automation*, pp. 490-498, ISBN: 0-7803-4300-X, Leuven, Belgium, May 1998

Shi, J.; Liu, H. & Bajcinca, N. (2008). Robust control of robotic manipulators based on integral sliding mode, *International Journal of Control*, Vol. 81, No. 10, October 2008, pp.1537–1548, ISSN : 0020-7179

Spong, M.(1987). Modeling and control of elastic joint robots, *IEEE Journal of Robotics and Automation*, Vol. RA-3, No.4, 1987, pp. 291-300

Spong, M.(1988). Variable structure control of flexible joint manipulators, *IEEE Journal of Robotics and Automation*, Vol. 3, No. 2, 1988, pp.57-64

Spong, M.(1989). Adaptive control of flexible joint manipulators, *Systems and Control Letters*, No.13, 1989, pp. 15-21

Stieber, M. ; Sachdev, S. & Lymer, J. (2000). Robotics architecture of the mobile servicing system for the international space station, *International Symposium of Robotics Research*, 2000, pp. 416-421

Tomei, P. (1991). A simple PD controller for robots with elastic joints, *IEEE Transactions on Automatic Control*, Vol. 36, No. 10, 1991, pp.1208-1213, ISSN: 0018-9286

Utkin, V.I. (1992). *Sliding Modes in Control and Optimization*, London, UK: Springer-Verlag

Utkin, V.I. & Shi, J. (1996). Integral sliding mode in systems operating under uncertainty conditions, *IEEE Conf. On Decision and Control*, pp. 4591-4596, ISBN: 0-7803-3590-2, Kobe (Japan), Dec. 1996

Utkin, V.I. ; Guldner, J. & Shi, J. (2009). *Sliding Mode Control in Electromechanical Systems*, Taylor & Francis publisher, (Second Edition)

Young, K.-K.D. (1978). Controller design for a manipulator using theory of variable structure systems, *IEEE Trans. on Systems, Man and Cybernetics*, Vol. 8, No. 2, Feb.1978, pp. 210-218, ISSN: 0018-9472

Young, K.-K.D. (1988). A variable structure model following control design for robotic applications, *IEEE Journal on Robotics and Automation*, Vol. 4, Oct. 1988, pp. 556-561, ISSN: 0882-4967

IntechOpen

Advances in Robot Manipulators

Edited by Ernest Hall

ISBN 978-953-307-070-4
Hard cover, 678 pages
Publisher InTech
Published online 01, April, 2010
Published in print edition April, 2010

The purpose of this volume is to encourage and inspire the continual invention of robot manipulators for science and the good of humanity. The concepts of artificial intelligence combined with the engineering and technology of feedback control, have great potential for new, useful and exciting machines. The concept of eclecticism for the design, development, simulation and implementation of a real time controller for an intelligent, vision guided robots is now being explored. The dream of an eclectic perceptual, creative controller that can select its own tasks and perform autonomous operations with reliability and dependability is starting to evolve. We have not yet reached this stage but a careful study of the contents will start one on the exciting journey that could lead to many inventions and successful solutions.

InTech Europe
University Campus STeP Ri
Slavka Krautzeka 83/A
51000 Rijeka, Croatia
Phone: +385 (51) 770 447
Fax: +385 (51) 686 166
www.intechopen.com

InTech China
Unit 405, Office Block, Hotel Equatorial Shanghai
No.65, Yan An Road (West), Shanghai, 200040, China
中国上海市延安西路65号上海国际贵都大饭店办公楼405单元
Phone: +86-21-62489820
Fax: +86-21-62489821

IntechOpen